Isomers of small Pb_n clusters ($n=2-15$): Geometric and electronic structures based on *ab initio* molecular dynamics simulations

C. Rajesh,[1] C. Majumder,[2,*] M. G. R. Rajan,[1] and S. K. Kulshreshtha[2]
[1]*Laboratory Nuclear Medicine Section, BARC, Trombay, Mumbai 400 085, India*
[2]*Chemistry Division, BARC, Trombay, Mumbai 400 085, India*
(Received 9 February 2005; revised manuscript received 19 August 2005; published 7 December 2005)

The geometric and electronic structure of the Pb_n clusters ($n=2-15$) has been calculated to elucidate its structural evolution and compared with other group-IV elemental clusters. The search for several low-lying isomers was carried out using the *ab initio* molecular dynamics simulations under the framework of the density functional theory formalism. The results suggest that unlike Si, Ge, and Sn clusters, which favor less compact prolate shape in the small size range, Pb clusters favor compact spherical structures consisting of fivefold or sixfold symmetries. The difference in the growth motif can be attributed to their bulk crystal structure, which is diamond-like for Si, Ge, and Sn but fcc for Pb. The relative stability of Pb_n clusters is analyzed based on the calculated binding energies and second difference in energy. The results suggest that $n=4$, 7, 10, and 13 clusters are more stable than their respective neighbors, reflecting good agreement with experimental observation. Based on the fragmentation pattern it is seen that small clusters up to $n=12$ favor monomer evaporation, larger ones fragment into two stable daughter products. The experimental observation of large abundance for $n=7$ and lowest abundance of $n=14$ have been demonstrated from their fragmentation pattern. Finally a good agreement of our theoretical results with that of the experimental findings reported earlier implies accurate predictions of the ground state geometries of these clusters.

DOI: 10.1103/PhysRevB.72.235411 PACS number(s): 73.22.−f, 36.40.Cg, 36.40.Qv, 36.40.Ei

I. INTRODUCTION

The realization of novel cluster assembled materials requires understanding of the fundamental properties of atomic clusters.[1–6] The structural and physico-chemical properties of the group IV elemental clusters have been the subjects of intense research because of the fundamental interest to understand their bonding and growth patterns and the possibility of applications in nanotechnology. Their growth behavior and the nature of bonding differ considerably as one goes down from C to Pb. During the past two decades a large number of experimental and theoretical studies[7–59] have been carried out in this direction. Much attention has been focused on understanding the structural similarities and differences among Si, Ge, Sn, and Pb clusters. The atomic structures of the group IV elemental clusters adopt geometries ranging from chain, fullerene cages and nanotubes for carbon[7] and non-compact prolate structures for Si, Ge, and Sn,[8–10,45–59] to compact structures for Pb. Structures of Si and Ge clusters progressively undergo rearrangements with an increase in size and transform into a 3D growth. Noda and co-workers[11,12] have reported mass spectrum of tin clusters that resembles those of Si_n and Ge_n clusters but different from that of Pb_n. Jarrold and coworkers[8–10,13,14] have characterized the structures of Si_n, Ge_n, Sn_n, and Pb_n clusters using ion mobility measurements. It is observed that the growth patterns of silicon, germanium and tin clusters adopt prolate structures in the small cluster region. However, for lead clusters, near-spherical structures have been predicted for all cluster sizes. So the transition to normal metal cluster growth in group IV elements occurs between tin and lead. Theoretical studies have been carried out for small tin clusters in order to understand the structure and bonding in these systems.[28,29] The results suggest that the strong covalent bond exists between Sn atoms in small clusters. In comparison to the other group IV elements, studies on the Pb clusters are few. Sattler *et al.*[15] have generated Pb_n clusters using the gas condensation technique. The time of flight mass spectrometric measurements indicated that $n=7$, 10, 13, 17, and 19 are more stable clusters. Comparison of mass abundance pattern of all group-IV elemental clusters revealed that Pb clusters behave differently from all others. In particular, the mass spectrum of Pb clusters rather resembles with that of inert gas atom Van der Waals clusters,[15,16] characteristic for close packed geometrical structures. Saito *et al.*[17] and Lai Hing *et al.*[18] subsequently carried out photoionization mass spectroscopy on Pb_n clusters. The ionization potentials measured of lead clusters[11,12] suggested that for ionization energy of 6.4 eV all lead clusters could be ionized except the atom (7.2 eV). Gantefor *et al.*,[19] Luder *et al.*,[20] and Negishi *et al.*[21] have recorded the photoelectron spectra of Sn_n and Pb_n ($n=2-20$) anion clusters. The detachment energies of the ground state cluster anions as well as the vertical detachment energies of the neutral clusters have been reported. The results from the photoelectron spectroscopy reveal that electronic structures of Sn_n and Pb_n clusters are different due to the directional and nondirectional nature of bonding, respectively. Experimental studies have been carried out for the fragmentation behavior of neutral and charged clusters of lead.[15,22,26] The results demonstrated the importance of electronic shell effects on the stability of neutral and charged clusters.

Although few experimental results have been reported for Pb_n clusters, theoretical studies are scarce. Balasubramanian *et al.*[30–37] have carried out a series of calculations on Pb clusters with particular emphasis on their spectroscopic prop-

erties. These computations were carried out using accurate techniques that included electron correlation effects and spin-orbit coupling simultaneously using a multi-reference relativistic configuration interaction method. Due to the requirement of extensive computation power, these studies were limited to very small clusters, i.e., up to $n=6$. The central feature of these studies showed that spin orbit coupling effect is quite important to describe the energetics of these clusters. The spin-orbit coupling can lower the atomization energies substantially; for example, the dissociation energy of Pb_2 is reduced by a factor of 2. This is a consequence of the fact that spin-orbit coupling lowers the energy of the atom substantially more than the cluster. In another theoretical study Molina *et al.*[38–40] have performed the total energy calculations of Pb_n clusters up to $n=14$ using the plane-wave-based pseudopotential method (PW-PSP) under the local spin density approximation scheme. They have obtained the atomization energies in very good agreement with that of experimental values. Very recently, Lai *et al.*[42] have calculated Pb_n clusters in the range of $3<n<56$ using the n-body Gupta potential[43] to account for the interactions between atoms in the cluster. In the present work we have performed *ab initio* molecular dynamics simulation using the density functional theory under the framework of generalized gradient approximation (GGA) to search for the low-lying isomeric structures and energetics of small size Pb_n ($n=2-15$) clusters. The analysis of the relative stabilities of these clusters has been carried out based on the total energies calculated that included spin orbit coupling term. The binding energies, second order energy difference, and their fragmentation behavior of these clusters have been analyzed. The results suggest that $n=4$, 7, 10, and 13 are more stable in this series, which is in agreement with the mass abundance pattern obtained from the photoionization experiment.[18] Further, in contrast to other group-IV elemental clusters, which adopt less compact prolate shape in the small size range, the ground state geometries of Pb_n ($n=2-15$) clusters favor compact and spherical structural growth pattern.

II. COMPUTATIONAL DETAILS

The geometry optimization of small Pb clusters was performed using the *ab initio* molecular dynamics simulation with projector augmented wave pseudopotential and plane wave basis set as implemented in VASP code.[65] The PAW pseudo-potential was generated taking scalar relativistic corrections into account. The spin polarized generalized gradient approximation[66] (GGA) has been used to calculate the exchange-correlation energy. Thus all relativistic effects except spin-orbit are included in the total energy calculation for different isomers of Pb_n clusters.

The cutoff energy of the plane waves is taken to be 98.0 eV. A simple cubic supercell of side 20 Å has been used and the Brillouin zone integrations are carried out using only the Γ point. In order to obtain few low lying isomers of Pb_n clusters, large number of initial geometries based on tetragonal, pentagonal or hexagonal growth and those reported for Si, Ge, and Sn clusters,[44–59] have been considered. The geometry optimization of each isomer was carried out till the forces on each atom becomes less than 0.005 eV/Å and the energy is converged to an accuracy of 0.0001 eV. In most cases the lowest energy isomer of each cluster was reconfirmed by comparing the energies of the isomers formed by adding or subtracting one atom with the corresponding nearest neighbor structures.

TABLE I. Comparison of calculated average binding energy (eV/atom) for dimer and bulk lead using the plane wave based pseudopotential method.

LDA[a]	GGA	PBE[b]	GGA/SO	Expt.	System
1.455	1.220	1.199	0.67	0.42[c]	Pb_2
3.798	3.000	2.949	2.07	2.03[d]	Bulk

[a]Local density approximation (Ref. 68).
[b]Perdew-Burke-Ernzerhof (Ref. 69).
[c]Reference 27.
[d]Reference 60.

Test calculations were done for dimer and bulk. In Table I we have summarized the results obtained using different exchange-correlation schemes.[67–69] In general, it is found that although the interatomic separations between Pb atoms agree with that of experimental values,[27,60] the binding energies are significantly overestimated. Further, Balasubramanian and coworkers have carried out several calculations to obtain the ground state geometries and spectroscopic properties of small lead clusters where in it is shown that these clusters have significant spin-orbit effect.[30–37] Motivated by these results test calculations were carried out for the dimer and bulk cohesive energy of Pb after incorporating the spin-orbit coupling effect. Significant improvement on the binding energies has been observed as can be seen from the values listed in Table I. The bulk cohesive energy using GGA scheme for exchange correlation is found to reduce from 3.0 to 2.07 eV/atom, which is in excellent agreement with the experimental values.[60] Since it is observed that spin-orbit effect in Pb clusters is non-negligible we have carried out the total energy calculations of the lowest energy isomers of Pb_n clusters including the spin-orbit coupling effect as employed in VASP software.[68]

In order to verify the quality of the plane wave based DFT results further calculations were performed using the localized Gaussian basis set as employed in Gaussian-98.[70] We have compared the total energies of few low-lying isomers using gradient corrected Becke exchange and Perdrew Wang exchange correlation[71] (B3PW91) method as well as MP2[72] (Moller Plesset correlation energy correction truncated to second order) method. Los Alamos relativistic effective core potentials with a double zeta valence[73] (LanL2DZ) were used as basis to take into account the scalar relativistic effects, including mass velocity and Darwin corrections for the heavy lead atom.

III. RESULTS AND DISCUSSION

A. Geometries

Figure 1 represents the low-lying isomers of Pb_n clusters. Although a large number of isomers have been considered

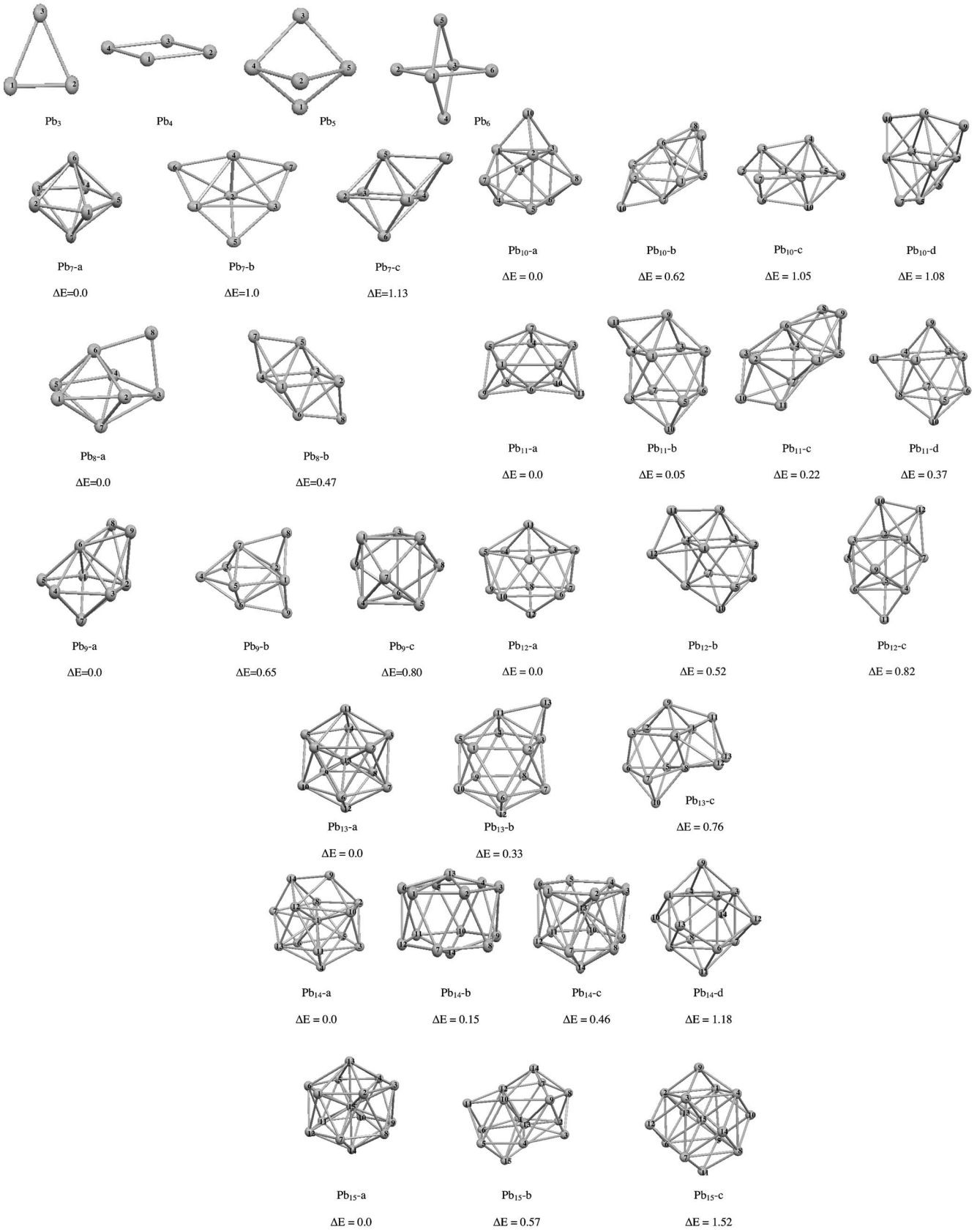

FIG. 1. Low-lying isomers (within 1.0 eV energy difference) of Pb_n (n=3–15) clusters calculated using the density functional theory and GGA approximation.

for each cluster, but for the sake of simplicity we have shown only those, which are within 1 eV energy more than from the lowest energy structure.

The Pb_2 dimer favors triplet spin configuration with bond length of 2.91 Å and the binding energy of 0.67 eV/atom. For Pb_3 cluster, equilateral triangle with triplet spin configuration shows the lowest energy structure with Pb-Pb bond length and average binding energy of 3.01 Å and 1.08 eV/atom, respectively. These results are in good agreement with those obtained by Balasubramanian and co-workers[32–37] using very accurate methods of CASSCF and MRSDCI, which shows 3.0 Å and 3.07 Å for the interatomic distances between Pb atoms in dimer and trimer, respectively. It needs to be mentioned that unlike other trimers of group-IV elements (Si, Ge and Sn), which form isosceles (C_{2v}) triangle and favors singlet as the lowest energy configuration,[28,45,51,52,57] Pb_3 favors equilateral triangle (D_{3h}) with triplet spin configuration, in consistent with the results obtained from infrared experiments.[27] Clusters with $n=4$ to $n=7$ have similar geometrical configurations as those found for the other group-IV elements. The lowest energy isomer of Pb_4 adopts rhombus geometry (D_{2h}) with Pb-Pb distance of 2.98 Å and an internal angle of 63.7°. The Pb_5 cluster shows capped bent rhombus as the ground state geometry, which can otherwise be viewed as an elongated trigonal bipyramid (D_{3h}). The shortest bond length between Pb atoms is found to be 2.97 Å. For Pb_6, several initial configurations viz., octahedron, trigonal prism, and trigonal bipyramid (TBP) with one additional atom capping edges or one of the triangular faces have been optimized. Both face and edge capped TBP relaxed to crossed rhombus (D_{4h}), which has been found to be the lowest energy configuration with Pb-Pb distances of 3.06 Å. Among different isomers of Pb_7, the pentagonal bipyramid (PBP) with D_{5h} symmetry was found to be the lowest energy structure. The Pb-Pb bond distance is estimated to be 3.19 Å. Other isomers, like bicapped TBP or capped octahedron showed significantly higher in energy as compared to the PBP structure and have been described in Fig. 1. For Pb_8 cluster, the lowest energy structure is found to favor an edge capped PBP. This is similar to the lowest energy isomer of Sn_8,[28] but different from that of Si_8 and Ge_8 which favor bicapped octahedron[48,51,52,57] as the lowest energy structure. The bicapped octahedron isomer (Pb_8-*b*) of Pb_8 lies about 0.42 eV high in energy. For Pb_9 cluster, several initial configurations were considered by capping the PBP, prism and octahedron geometries. The lowest energy isomer of the Pb_9 cluster is found to favor bicapped PBP structure with two capping atoms placed at the adjacent triangular faces on the same side of the pentagon. Another isomer having tricapped prism (Pb_9-*b*) configuration shows 0.24 eV higher in energy than the lowest energy isomer. For Pb_{10}, initial geometries based on capping different faces of octahedron, PBP and prism or antiprism structures were considered. The lowest energy structure is found to favor capped trigonal prism as shown in Fig. 1. Two other isomers based on tricapped PBP (Pb_{10}-*b*) and pentagonal antiprism (optimized into two fused octahedrons, Pb_{10}-*c*) show 0.52 eV and 1.08 eV higher in energy with respect to the lowest energy structure, respectively. The tetracapped octahedron (T_d,Pb_{10}-*d*) structure is found to be 1.37 eV higher in energy.

For Pb_{11} cluster, several initial configurations were generated. These were based on capping different faces of PBP structures and those previously reported for other group-IV clusters and by subtracting one or two atoms from Pb_{12} or Pb_{13} icosahedron structures. Two isomeric structures, one based on pentagonal base and the other based on tetragonal base were found to lie with in 0.1 eV energy difference. The lowest energy structure (Pb_{11}-*a*) is obtained starting from tetracapped PBP where all four capping atoms were placed on the same side of the base pentagon, which after relaxation adopts icosahedron motif as shown in Fig. 1. The next higher energy isomer (Pb_{11}-*b*), which lies very close in energy to that of the lowest energy isomer, shows bicapped tetragonal antiprism with additional Pb atom capping one of the triangular faces. The other isomer of tetracapped PBP (Pb_{11}-*c*), where two Pb atoms are capping from opposite side of the PBP is 0.21 eV higher in energy. In general, comparison of total energies between the low lying isomers of Pb_{11} cluster suggests that the potential energy surface is rather flat and structural transition might occur at higher temperatures or even by using different approximation in the exchange correlation energy functional. In fact under MP2, the lowest energy structure of Pb_{11} cluster favor tricapped tetragonal antiprism, which in plane wave based pseudo-potential method was 0.1 eV higher in energy than the lowest energy isomer with pentagonal symmetry (Pb_{11}-*b*). In this context it is worth to mention that for Si_{11} cluster, the existence of multiple nearly degenerate low-energy isomers was found, which has shown structural transition of the lowest energy isomer depending upon the exchange-correlation functions.[57]

For Pb_{12} cluster, several isomers based on tetragonal, pentagonal and hexagonal structural motifs were taken into consideration to search for the low-lying isomers. The lowest energy structure shows empty cage distorted icosahedron. The next low-lying isomer is a tetracapped tetragonal antiprism, which is 0.43 eV higher in energy. Both these structures can be viewed as a sequential addition of one more Pb atom to Pb_{11}-*a* and Pb_{11}-*b* isomers of Pb_{11}. In this context it is worth to mention that, while in the case of Pb_{11} cluster the lowest energy isomer which forms a pentagonal base is only 0.1 eV lower than the next lower isomer of tricapped tetragonal antiprism, but for Pb_{12} the difference between the pentagonal and tetragonal structure increases significantly (0.43 eV), imply the trend for an icosahedral growth for larger size clusters.

For Pb_{13}, isomers like capped icosahedron, Pb encapsulated icosahedron and a few low lying isomers of the group-IV elemental clusters having less compact prolate shape geometries were considered as initial geometries. Slightly distorted Pb atom encapsulated icosahedron was found to be the most stable isomer while the low lying isomers of the other group-IV elements were found to be at least 0.38 eV higher in energy. This is significantly different than what is commonly observed for other group-IV clusters. The difference in the structural motif in the small clusters can be related to their bulk structures, which for Pb is a compact fcc and for others it is less compact tetragonal.[60]

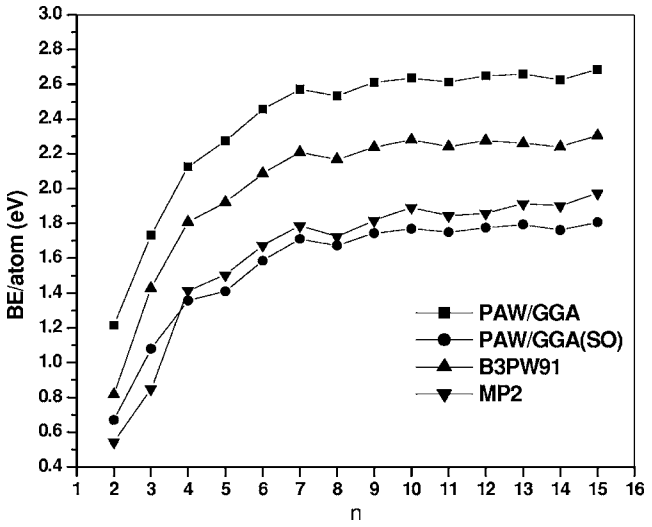

FIG. 2. Binding energy per atom of Pb_n clusters as a function of cluster size.

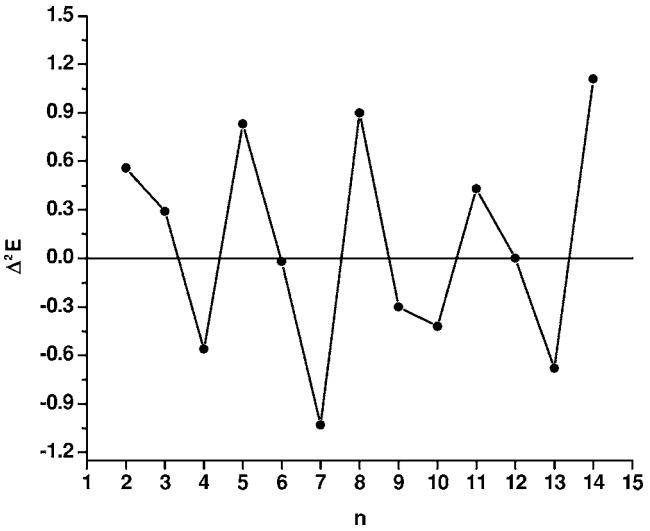

FIG. 3. Plot of second order difference in total energy as a function of cluster size.

Other isomers, like cuboctahedron or decahedron show significantly higher energy (~1.6–1.7 eV). Previous studies[61] have shown that elements with large compressibilites are more likely to exhibit spherical growth of their clusters. The higher compressibility of Pb as compared to those for Si, Ge, and Sn further establish its compact icosahedral growth pattern.

For Pb_{14}, several isomers, viz. capped icosahedron, hexagonal layered and fcc structure (bulk cut) were optimized. An icosahedron with the additional atom capping one of the triangular faces of the Pb_{13} cluster from outside was found to show the lowest energy structure. The next low lying isomer of Pb_{14} (Pb_{14}-*b*) shows similar trend of the close packing by adding one Pb atom in each of the pentagonal plane resulting in hexagonal antiprism having an encapsulated Pb atom and one Pb atom capping the hexagonal face. The energy difference of the capped hexagonal antiprism isomer with respect to the lowest energy isomer is 0.19 eV.

For Pb_{15} cluster, initial configurations were generated based on the pentagonal and hexagonal structural motifs. Some of these consist of capping icosahedrons or hexagonal antiprism structures as well as encapsulated hexagonal prisms etc. Comparison of the total energies among all these isomers after geometry relaxation suggests that the ground state geometry of the Pb_{15} cluster favors encapsulated hexagonal antiprism structure. This further corroborates the compact structural motif of the Pb clusters as compact structure, which bears a signature of metallic behavior, which is significantly different from that of other group-IV elemental clusters.

B. Energetics

In order to understand the relative stability of these clusters we have estimated the average binding energies, second order difference in energy and the fragmentation behavior based on the total energies obtained for the lowest energy isomer. Figure 2 represents the average binding energies as a function of cluster size. We have compared the binding energies of Pb cluster at different levels of theoretical models. The average binding energy of these clusters is calculated as

$$\mathrm{BE}(\mathrm{Pb}_n) = -[E(\mathrm{Pb}_n) - n \times E(\mathrm{Pb})]/n.$$

It is clear from this figure that both PAW/GGA (without spin-orbit correction) and B3PW91 show significantly higher binding energies as compared to the results obtained by incorporating the spin-orbit correction in PAW/GGA method. Therefore, total energy calculations including the spin-orbit effects are extremely important for these clusters. For smaller size clusters (Pb_2 and Pb_3) although the binding energies obtained from MP2 method are closer to the experimental values[26,27] (0.42 and 0.77 eV/atom for Pb_2 and Pb_3, respectively) however, they overestimate as the size increases. This is evident from the fact that for $n=15$ the binding energy obtained from MP2 is already within 97% of the bulk. On the other hand, though for smaller clusters the binding energies obtained from the PAW/GGA (SO) calculations are higher as compared to the experimental values, the cohesive energy of the Pb bulk calculated under PAW/GGA (SO) method shows 2.07 eV/atom, in good agreement with experimental observation.[60] Therefore, it is expected that under PWA/GGA (SO) method the binding energy values will converge with experiment as the size of the cluster grows. For small clusters in the range up to $n=15$, the trend in the binding energy curve shows that in general it increases as the cluster size grows with small humps or dips for specific size of clusters indicating their relative stabilities. Accordingly, small humps at $n=7$, 10, and 13 as shown in Fig. 2, reflect their higher stabilities over other clusters. These results are in excellent agreement with the experimentally observed mass abundance pattern[13–15] of Pb_n clusters.

Magic clusters are those, which show higher stability as compared to its nearest neighbors. Based on the calculated total energies of different clusters one can search for stable clusters by calculating the second energy difference in energy, which has been calculated as

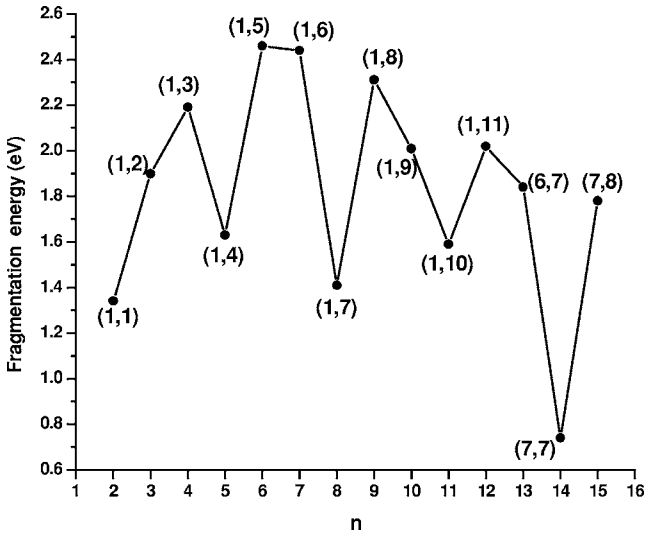

FIG. 4. The lowest energy fragmentation channels of Pb_n clusters. The numbers in the brackets indicate the product fragments.

$$\Delta^2 E = [2^* E(\mathrm{Pb}_n) - E(\mathrm{Pb}_{n+1}) - E(\mathrm{Pb}_{n-1})].$$

From the above expressions it is clear that the clusters, which have negative values of $\Delta^2 E$ are more stable than its nearest neighbors. We have plotted the $\Delta^2 E$ for Pb_n clusters as a function of cluster size as shown in Fig. 3. Expectedly, it is found that clusters with $n=4$, 7, 10, and 13 are relatively more stable than their nearest neighbors. This is in agreement with previous experimental observations.[13–15]

It is known that in general the stability of the atomic clusters is governed either by electronic shell model (commonly observed for alkali metal clusters) or by geometrical close packing model (commonly observed for inert gas clusters).[62,63] According to the electronic shell model, clusters with 2, 8, 18, 20, 34, 40, etc. numbers of electrons are more stable. However, the stability order under the geometrical close packed structures favors clusters with 7, 13, 19, 23, etc. number of atoms.[62,63] For covalent clusters, due to directional bonding, neither of these two models is obeyed. This fact is reflected in the magic stability pattern of Si clusters where $n=4,6,7,10,12$ are more stable than their nearest neighbors.[64] Interestingly, the stability pattern of Pb clusters shows $n=4$, 7, 10, and 13 are magic. Although the higher stabilities of $n=7,13$ of Pb clusters can be explained by geometrical close packing however, higher stability of $n=10$ could be a resultant of both electronic shell filling as well as compact trigonal prism geometries.

C. Fragmentation behavior

We have analyzed the fragmentation behavior of the Pb_n clusters. Although it is known that the fragmentation process involves a dissociation barrier and entropy or free energy changes, in the present work we have assumed the fragmentation path by only looking at the total energy of the parent and daughters thereby leading to infer about the relative stability of these clusters in the ground state. For this purpose the fragmentation energies have been calculated for all possible channels, which can be expressed as

TABLE II. Fragmentation behavior of Pb_n clusters. The bold numbers for the fragmentation energy represent the lowest fragmentation channel.

n	p	$n-p$	E_f	n	p	$n-p$	E_f
2	**1**	**1**	**1.34**	12	**1**	**11**	**2.02**
3	**1**	**2**	**1.90**	12	2	10	2.27
4	**1**	**3**	**2.19**	12	3	9	2.38
4	2	2	2.75	12	4	8	2.50
5	**1**	**4**	**1.63**	12	5	7	2.28
5	2	3	2.48	12	6	6	2.26
6	**1**	**5**	**2.46**	13	1	12	2.02
6	2	4	2.75	13	2	11	2.70
6	3	3	3.04	13	3	10	2.39
7	**1**	**6**	**2.44**	13	4	9	2.21
7	2	5	3.56	13	5	8	2.89
7	3	4	3.29	13	**6**	**7**	**1.84**
8	**1**	**7**	**1.41**	14	1	13	1.34
8	2	6	2.51	14	2	12	2.02
8	3	5	3.07	14	3	11	2.14
8	4	4	2.51	14	4	10	1.54
9	**1**	**8**	**2.31**	14	5	9	1.92
9	2	7	2.38	14	6	8	1.77
9	3	6	2.92	14	**7**	**7**	**0.74**
9	4	5	3.19	15	1	14	2.45
10	**1**	**9**	**2.01**	15	2	13	2.45
10	2	8	2.98	15	3	12	2.57
10	3	7	2.49	15	4	11	2.40
10	4	6	2.74	15	5	10	2.36
10	5	5	3.57	15	6	9	1.91
11	**1**	**10**	**1.59**	15	**7**	**8**	**1.78**
11	2	9	2.26				
11	3	8	2.67				
11	4	7	1.89				
11	5	6	2.70				

$$E_f(\mathrm{Pb}_n) = E(\mathrm{Pb}_n) - E(\mathrm{Pb}_{n-p}) - E(\mathrm{Pb}_p).$$

For the sake of simplicity we have plotted the fragmentation energies of the lowest energy channels as a function of the cluster size as shown in Fig. 4. The complete list of the fragmentation energies for all possible channels is provided in Table II. From Fig. 4, it is clear that while smaller size clusters up to $n=12$, favor monomer evaporation as the lowest energy fragmentation channel, larger clusters ($n>12$) favor to dissociate into two stable daughter cluster. For $n=13$, 14, and 15, the lowest fragmentation channel was found to be (6, 7), (7, 7), and (7, 8), respectively. The higher abundance of Pb_7 in mass spectrometry experiment[13–15] can therefore be a consequence of the favored fragmentation channel of larger clusters into $n=7$ as one of the fragmented species. Duncan *et al.*[18] in their photo ionization experiment have noticed that $n=14$ is missing in the mass spectrum. This observation can lead to two inferences. The first reason could

be due to the very high stability of Pb_{14} cluster for which the ionization potential is higher than the ionizing energy of the photon or due to very low fragmentation energy, which leads to fragment the Pb_{14} cluster as soon as they are formed. From our study on the binding energy and fragmentation behavior of Pb_n clusters ($n=2-15$) we conclude that the later reason is correct. It has been estimated that the fragmentation energy of Pb_{14} cluster into two Pb_7 daughter cluster is 0.74 eV (Table II). The lowest fragmentation energy of Pb_{14} cluster as compared to the others in the series is attributed to the production of two magic clusters of Pb_7 and further explains its unavailability in the photoionization experiment.

IV. CONCLUSION

The geometric and electronic structure of Pb_n clusters have been investigated using the *ab initio* molecular dynamics simulation. Plane-wave-based pseudo-potential method under the GGA scheme was used to optimize the geometry of several isomers. Further, spin-orbit coupling effect was included to calculate the total energy of the lowest energy isomers. The relative stability of few low-lying isomers was verified by more accurate quantum chemical methods based on hybrid energy functional as well as at the MP2 level theory under the LCAO-MO methods. It is found that the binding energies are significantly improved after the inclusion of spin-orbit effect term. In fact for small clusters like Pb_2, the binding energy has been reduced to half. Several low-lying isomers have been identified based on tetragonal, pentagonal and hexagonal configurations. The ground state geometries of Pb_n clusters up to $n=7$ show similarities with other group-IV clusters. For $n=8-10$, slow transition towards close packed geometries has been observed. From $n=11$ onwards, the lowest energy structures evolved with close packed structures having five or sixfold symmetry. From $n=13$, encapsulation of a Pb atom inside the spherical cage of icosahedron initiates, which starts at a much larger size for Si clusters. Based on these results we infer that unlike other group-IV clusters the compact spherical structures are formed for Pb cluster even at smaller size range. This trend is in agreement with their bulk structures, which is diamond like for Si, Ge, and Sn and fcc for Pb. This nature can further be attributed to the higher compressibility of lead over other elements in group IV. The relative stability of these clusters has been analyzed based on their average binding energy, second order difference in energy, and fragmentation pattern. The results reveal that $n=4$, 7, 10, and 13 atom clusters have higher stability than the other clusters in this series. This is in excellent agreement with the experimentally observed mass abundance pattern reflecting the confidence in the predicted ground state geometries of these clusters presented in this work. The fragmentation behavior suggests that while small clusters favor monomer evaporation as the lowest fragmentation energy channel, larger clusters ($n>12$) favor to dissociate into two stable daughter clusters. The large abundance of $n=7$ and absence of $n=14$ clusters in the photoionization experiment has been clearly demonstrated from the fragmentation analysis of the Pb_{14} cluster. Based on our stability analysis of Pb_n clusters and the available experimental results, which suggests that $n=4,7,10,13$ are magic, we infer that both electronic and geometric packing are responsible for their stability order of these clusters.

ACKNOWLEDGMENTS

We are thankful to the members of the Computer Division, BARC, for their kind cooperation during this work. We gratefully acknowledge the help of Dr. Naresh Patwari, IIT Mumbai, for his cooperation to carry out the LCAO-MO calculations using the Gaussian software.

*Corresponding author. Email address: chimaju@magnum.barc.ernet.in

[1] V. Kumar, K. Esfarjani, and Y. Kawazoe, in *Clusters and Nanomaterials*, Springer Series in Cluster Physics, edited by Y. Kawazoe and K. Ohno (Springer, Heidelberg, 2002), p. 9.
[2] A. Kasuva, R. Sivamohan, Y. A. Barnakov, I. M. Dmitruk, T. Nirasawa, V. R. Romanyuk, V. Kumar, S. V. Mamykin, K. Tohji, B. Jeyadevan, T. Kudo, O. Terasaki, Z. Liu, R. V. Belosludov, V. Sundararajan, and Y. Kawazoe, Nat. Mater. **3**, 99 (2004).
[3] G. Seifert, Nat. Mater. **3**, 77 (2004).
[4] V. Kumar and Y. Kawazoe, Phys. Rev. Lett. **87**, 045503 (2001).
[5] S. N. Khanna and P. Jena, Phys. Rev. Lett. **69**, 1664 (1992).
[6] B. K. Rao, P. Jena, M. Manninen, and R. M. Nieminen, Phys. Rev. Lett. **58**, 1188 (1987).
[7] G. Von Helden, M. T. Hsu, N. Gotts, and M. T. Bowers, J. Phys. Chem. **97**, 8182 (1993).
[8] M. F. Jarrold and V. A. Constant, Phys. Rev. Lett. **67**, 2994 (1991).
[9] M. F. Jarrold and J. E. Bower, J. Chem. Phys. **96**, 9180 (1992).
[10] J. M. Hunter, J. L. Fye, M. F. Jarrold, and J. E. Bower, Phys. Rev. Lett. **73**, 2063 (1994).
[11] M. Watanabe, Y. Saito, S. Nishigaki, and T. Noda, Jpn. J. Appl. Phys., Part 1 **27**, 427 (1988).
[12] Y. Saito and T. Noda, Z. Phys. D: At., Mol. Clusters **12**, 225 (1989).
[13] A. A. Shvartsburg and M. F. Jarrold, Phys. Rev. A **60**, 1235 (1999).
[14] A. A. Shvartsburg and M. F. Jarrold, Chem. Phys. Lett. **317**, 615 (2000).
[15] K. Sattler, J. Muhlbach, O. Echt, P. Pfau, and E. Recknagel, Phys. Rev. Lett. **47**, 160 (1981).
[16] O. Echt, K. Sattler, and E. Recknagel, Phys. Rev. Lett. **47**, 1121 (1981).
[17] Y. Saito, K. Yamauchi, K. Mihama, and T. Noda, Jpn. J. Appl. Phys., Part 1 **21**, L396 (1982).
[18] K. LaiHing, R. G. Wheeler, W. L. Wilson, and M. A. Duncan, J. Chem. Phys. **87**, 3401 (1987).
[19] G. Gantefor, M. Gausa, K. H. Meiwes-Broer, and H. O. Lutz, Z.

Phys. D: At., Mol. Clusters **12**, 405 (1989).
[20] Ch. Luder and K. H. Meiwes-Broer, Chem. Phys. Lett. **294**, 391 (1998).
[21] Y. Negishi, H. Kawamata, A. Nakajima, and K. Kaya, J. Electron Spectrosc. Relat. Phenom. **106**, 117 (2000).
[22] A. Hoareau, P. Melinon, B. Cabaud, D. Rayone, B. Tribollet, and M. Broyer, Chem. Phys. Lett. **143**, 602 (1988).
[23] M. Abshagen, J. Kowalski, M. Meyberg, G. Zu Putlitz, J. Slaby, and F. Trager, Chem. Phys. Lett. **174**, 455 (1990).
[24] I. Rabin, W. Schulze, and B. Winter, Phys. Rev. B **40**, 10282 (1989).
[25] P. Jena, B. K. Rao, and R. M. Nieminen, Solid State Commun. **59**, 509 (1986).
[26] R. W. Farley, P. Ziemann, and A. W. Castleman, Z. Phys. D: At., Mol. Clusters **14**, 353 (1989).
[27] D. D. Stranz and R. K. Khanna, J. Chem. Phys. **74**, 2116 (1981).
[28] C. Majumder, V. Kumar, H. Mizesuki, and Y. Kawazoe, Phys. Rev. B **64**, 233405 (2001).
[29] K. Joshi, D. G. Kanhere, and S. A. Blundell, Phys. Rev. B **66**, 155329 (2002).
[30] K. Balasubramanian, Chem. Rev. (Washington, D.C.) **90**, 83 (1990).
[31] K. S. Pitzer and K. Balasubramanian, J. Phys. Chem. **86**, 3068 (1982); K. Balasubramanian and K. S. Pitzer, J. Chem. Phys. **78**, 321 (1983).
[32] K. Balasubramanian and D. Majumdar, J. Chem. Phys. **115**, 8795 (2001).
[33] D. Dai and K. Balasubramanian, J. Chem. Phys. **96**, 8345 (1992).
[34] D. Dai and K. Balasubramanian, J. Phys. Chem. **96**, 9236 (1992).
[35] D. Dai and K. Balasubramanian, Chem. Phys. Lett. **271**, 118 (1997).
[36] C. Zhao and K. Balasubramanian, J. Chem. Phys. **116**, 10287 (2002).
[37] K. Balasubramanian, J. Chem. Phys. **85**, 3401 (1986).
[38] B. Wang, L. M. Molina, M. J. Lopez, A. Rubio, J. A. Alonso, and M. J. Stott, Ann. Phys. (N.Y.) **7**, 107 (1998).
[39] L. M. Molina, M. J. Lopez, A. Rubio, L. C. Balbas, and J. A. Alonso, Adv. Quantum Chem. **33**, 329 (1999).
[40] M. P. Iniguez, M. J. Lopez, J. A. Alonso, and J. M. Soler, Z. Phys. D: At., Mol. Clusters **11**, 163 (1989).
[41] A. M. Mazzone, Phys. Rev. B **54**, 5970 (1996).
[42] S. K. Lai, P. J. Hsu, W. K. Liu, and M. Iwamatsu, J. Chem. Phys. **117**, 10175 (2002).
[43] R. P. Gupta, Phys. Rev. B **23**, 6265 (1981).
[44] K. Raghavachari and V. Logovinsky, Phys. Rev. Lett. **55**, 2853 (1985).
[45] K. Raghavachari, J. Chem. Phys. **84**, 5672 (1986).
[46] K. Raghavachari and C. M. Rohlfing, J. Chem. Phys. **89**, 2219 (1988).
[47] C. M. Rohlfing, and K. Raghavachari, Chem. Phys. Lett. **167**, 559 (1990).
[48] K. Raghavachari and C. M. Rohlfing, Chem. Phys. Lett. **94**, 3670 (1991).
[49] K. Raghavachari and C. M Rohlfing, Chem. Phys. Lett. **198**, 521 (1992).
[50] B. Liu., Z.-Y. Lu, B. Pan, C.-Z. Wang, K.-M. Ho, A. A. Shvartsburg, and M. F. Jarrold, J. Chem. Phys. **109**, 9401 (1998).
[51] K.-M. Ho, A. A. Shvartsburg, B. Pan, Z.-Y. Lu, C.-Z. Wang, J. G. Wacker, J. L. Fye, and M. F. Jarrold, Nature (London) **392**, 582 (1998).
[52] A. A. Shvartsburg, Bei Liu, Zhong-Yi Lu, Cai-Zhuang Wang, Martin F. Jarrold, and Kai-Ming Ho, Phys. Rev. Lett. **83**, 2167 (1999).
[53] J. Mitas, J. C. Grossmann, I. Stich, and J. Tobik, Phys. Rev. Lett. **84**, 1479 (2000).
[54] E. Honea, A. Ogura, A. Murray, K. Raghavachari, W. O. Senger, M. F. Jarrold, and W. L. Brown, Nature (London) **366**, 42 (1993).
[55] S. Li, R. J. Van Zee, W. Weltner Jr., and K. Raghavachari, Chem. Phys. Lett. **243**, 275 (1995).
[56] C. Xu, T. R. Taylor, G. R. Burton, and D. M. Neumark, J. Chem. Phys. **108**, 1395 (1998).
[57] Xiaolei Zhu and X. C. Zeng, J. Chem. Phys. **118**, 3558 (2003).
[58] G. R. Burton, C. Xu, C. C. Arnold, and D. M. Neumark, Chem. Phys. **104**, 2757 (1996).
[59] S. Ogut and J. R. Chelikowsky, Phys. Rev. B **55**, R4914 (1997).
[60] C. Kittel, *Introduction to Solid State Physics*, 7th ed. (Wiley & Sons, New York, 1996), p. 57.
[61] V. Kumar and Y. Kawazoe, Phys. Rev. B **63**, 075410 (2001).
[62] W. A. de Heer, Rev. Mod. Phys. **65**, 611 (1993).
[63] Matthias Brack, Rev. Mod. Phys. **65**, 677 (1993).
[64] T. P. Martin and H. Schaber, J. Chem. Phys. **83**, 855 (1985).
[65] Vienna *ab initio* simulation package, Technische Universitat Wien, 1999; G. Kresse and J. Hafner, Phys. Rev. B **47**, 558 (1993); G. Kresse and J. Furthmuller, Phys. Rev. B **54**, 11 169 (1996).
[66] P. E. Blochl, Phys. Rev. B **50**, 17953 (1994); G. Kresse and J. Joubert, Phys. Rev. B **59**, 1758 (1999).
[67] J. P. Perdew, in *Electronic: Structure of Solids 1991*, edited by P. Ziesche and H. Eschrig (Akademie Verlag, Berlin, 1991), p. 11.
[68] D. M. Ceperley and B. J. Alder, Phys. Rev. Lett. **45**, 566 (1980); J. P. Perdew and A. Zunger, Phys. Rev. B **23**, 5048 (1981).
[69] J. P. Perdew, K. Burke, and M. Ernzerhof, Phys. Rev. Lett. **77**, 3865 (1996).
[70] M. J. Frisch *et al.*, Computer code Gaussian 98, revision A.6, Gaussian, Inc., Pittsburgh PA, 1998.
[71] A. D. Becke, Phys. Rev. A **38**, 3098 (1988); A. D. Becke, J. Chem. Phys. **98**, 5648 (1993); J. P. Perdrew and Y. Wang, Phys. Rev. B **45**, 13224 (1992).
[72] C. Moller and M. S. Plesset, Phys. Rev. B **46**, 618 (1934).
[73] W. R. Wadt and P. J. Hay, J. Chem. Phys. **82**, 284 (1985); P. J. Hay and W. R. Wadt, *ibid.* **82**, 270 (1985); **82**, 299 (1985).